Estimation of the bias of the Minimum Variance technique in the determination of magnetic clouds global quantities and orientation

A.M. Gulisano [a,*], S. Dasso [a,b,1], C.H. Mandrini [a,1], P. Démoulin [c]

[a] *Instituto de Astronomía y Física del Espacio, CONICET-UBA, CC. 67, Suc. 28, 1428 Buenos Aires, Argentina*
[b] *Departamento de Física, Facultad de Ciencias Exactas y Naturales, UBA, 1428 Buenos Aires, Argentina*
[c] *Observatoire de Paris, Meudon, LESIA, UMR 8109 (CNRS), F-92195 Meudon Cedex, France*

Abstract

Magnetic clouds (MCs) are highly magnetized plasma structures that have a low proton temperature and a magnetic field vector that rotates when seen by a heliospheric observer. More than 25 years of observations of magnetic and plasma properties of MCs at 1 AU have provided significant knowledge of their magnetic structure. However, because in situ observations only give information along the trajectory of the spacecraft, their real 3D magnetic configuration remains still partially unknown. We generate a set of synthetic clouds, exploring the space of parameters that represents the possible orientations and minimum distances of the satellite trajectory to the cloud axis, p. The synthetic clouds have a local cylindrical symmetry and a linear force-free magnetic configuration. From the analysis of synthetic clouds, we quantify the errors introduced in the determination of the orientation/size (and, consequently, of the global magneto-hydrodynamic quantities) by the Minimum Variance method when p is not zero.
© 2007 COSPAR. Published by Elsevier Ltd. All rights reserved.

Keywords: MHD and plasmas; Interplanetary space; Solar wind

1. Introduction

Magnetic clouds (MCs) are highly magnetized plasma structures that have a low proton temperature and a magnetic field vector that rotates when seen by a heliospheric observer.

Even though MCs have been studied for more than 25 years, there is no agreement about their true magnetic configurations. This is mainly because the magnetic field data retrieved in situ by a spacecraft correspond only to the one dimensional cut along its trajectory and, thus, it is necessary to make some assumptions to infer the cloud 3D structure from observations.

Different distributions of the magnetic field inside the MC have been considered by several authors. A cylindrical magnetic configuration with a linear force-free field was proposed by Goldstein (1983), the so-called Lundquist's model (Lundquist, 1950). This model has been considered as a relatively good approximation of the field distribution inside MCs by several authors (e.g., Burlaga and Behannon, 1982; Lepping et al., 1990; Burlaga, 1995; Burlaga et al., 1998; Lynch et al., 2003, 2005; Dasso et al., 2005b, 2006). However, many other different models have been also used to describe the magnetic structure of MCs. Some authors take a cylindrical shape for the cloud, but consider a non-linear force-free field (Farrugia et al., 1999). Mulligan et al. (1999); Hidalgo et al. (2000, 2002); and Cid et al. (2002) propose different models with non-force-free fields. Non-cylindrical static models have been also applied to MCs (e.g., Hu and Sunnerup, 2001; Vandas et al., 2003; Hu and Dasgupta, 2005).

---

* Corresponding author. Tel.: +54 11 47832642; fax:+ 54 11 47868114.
 E-mail address: agulisano@iafe.uba.ar (A.M. Gulisano).
[1] Member of the Carrera del Investigador Científico, CONICET, Argentina.

From in situ observations and assumptions on the magnetic distribution inside the MC, it is possible to estimate some global magnetohydrodynamic quantities, such as magnetic fluxes and helicity (e.g., Dasso et al., 2003; Mandrini et al., 2005; Gulisano et al., 2005; Attrill et al., 2006; Dasso et al., 2006). In order to obtain good estimations of these quantities, it is necessary to find the correct MC orientation, improve the estimation of its size and components of **B** in the cloud frame.

The Minimum Variance method (MV) has been extensively used to find the orientation of structures in the interplanetary medium (see e.g., Sunnerup and Cahill, 1967; Burlaga and Behannon, 1982). The Minimum Variance method applied to the observed temporal series of the magnetic field can estimate quite well the orientation of the cloud axis, when the distance between the axis and the spacecraft trajectory in the MC (the impact parameter, p) is low with respect to the cloud radius (see e.g., Klein and Burlaga, 1982; Bothmer and Schwenn, 1998; Gulisano et al., 2005). The MV method has two main advantages with respect to other more sophisticated techniques that are also used to find the orientation of an MC: (1) it is relatively easy to apply, and (2) it makes a minimum number of assumptions on the magnetic configuration. Unfortunately, when p is significant, the MV approach is no longer accurate and it provides an orientation which deviates from the real one. However, quantitative estimations of the errors in the cloud orientation given by the MV technique for finite values of p have not been exhaustively done.

Some authors have used the MV technique to determine the orientation of MCs (e.g., Klein and Burlaga, 1982; Bothmer and Schwenn, 1998; Farrugia et al., 1999; Xiao et al., 2004; Gulisano et al., 2005). Other authors use the MV method to get a first order approximation for the MC orientation. Then, they use this estimation as a seed in a non-linear least-squares fit of a magnetic model to the data. This approach is expected to improve the cloud orientation and allows to find the value of p (e.g., Lepping et al., 1990, 2003, 2006; Dasso et al., 2005b). However, we notice that the solutions of this fitting can depend on the seed introduced as input. Moreover, these methods need important additional hypothesis to build a magnetic model (e.g., Shimazu and Marubashi, 2000; Mulligan et al., 2001; Hidalgo et al., 2002; Cid et al., 2002; Hu and Sunnerup, 2002; Lynch et al., 2003; Hidalgo, 2003). Conversely, the MV method just requires a well ordered large scale variance of **B** in the three spatial directions. Several of these different sophisticated techniques have been compared analyzing the output of numerical simulations of MCs (Riley et al., 2004). These authors found that these techniques give orientations that differ from the real ones by ∼10° to 30° in the latitude angle of the MC axis and by ∼10° in the longitude angle, even for low values of p/R (where R is the cloud radius). Larger differences in the MC orientation are found for larger values of p/R (see Tables I and II in Riley et al., 2004).

In order to estimate the error introduced by the Minimum Variance method, we generate a set of synthetic clouds, considering a cylindrical geometry and a linear force-free field (Lundquist's model, 1950). The clouds in the set have different orientations and p. We perform a Minimum Variance study in a similar way as the one applied to cloud observations from one spacecraft. The direction associated to the intermediate eigenvalue gives the estimated direction of the MC axis (see Section 2). Assuming a null impact parameter, we estimate the MC radius. Then, we fit a Lundquist's model to the synthetic data to determine the physical parameters (magnetic field strength and twist) keeping the orientation fixed (as given by the MV method). This last step is done to estimate the propagation of the errors in the axis orientation and $p = 0$ in the global quantities (magnetic fluxes and helicity). We also provide an estimation of p/R from the data rotated to the frame of the MV eigenvectors. This permits us to correct the values of the global quantities when p/R is finite. In Section 2, we describe briefly the Minimum Variance method applied to magnetic clouds, the physical model, and the global quantities. In Section 3, we explain how we generate the synthetic clouds. In Section 4, we compare the results of our MV analysis with the original parameters that characterize the generated clouds. Finally, in Section 5, we summarize our findings and conclude.

2. Minimum Variance technique

2.1. The method

The MV method finds the direction **n** in which the projection of a series of N vectors has a minimum mean quadratic deviation and also provides the directions of intermediate and maximum variance (e.g., Sonnerup and Scheible, 1998). This method is very useful to determine the orientation of structures that present three clearly distinguished variance directions. In particular, when this method is applied to the magnetic field **B**, the mean quadratic deviation in a generic direction **n** is

$$\sigma_n^2 = \frac{1}{N} \sum_{k=1}^{N} (\boldsymbol{B^k} . \boldsymbol{n} - \langle \boldsymbol{B} \rangle . \boldsymbol{n})^2 \tag{1}$$

where $\boldsymbol{B^k}$ corresponds to each element (k) of the magnetic field series. The field mean value is

$$\langle \boldsymbol{B} \rangle = \frac{1}{N} \sum_{k=1}^{N} \boldsymbol{B^k} \tag{2}$$

The MV method finds the direction where σ_n^2 is minimum under the constraint $|\boldsymbol{n}| = 1$. The Lagrange multipliers variational method can be used in this determination. λ is the Lagrange multiplier in the following system of equations:

$$\frac{\partial}{\partial n_i} \{ \sigma_n^2 - \lambda(|\boldsymbol{n}|^2 - 1) \} = 0 \tag{3}$$

where $i = 1, 2, 3$ corresponds to the three components of $\boldsymbol{n}$. After applying Eq. (3), the resulting set of three equations can be written in matrix form as

$$\sigma_n^2 n_j = \sum_{i=1}^{3} (m_{ij} n_i) = \lambda n_j \tag{4}$$

where

$$m_{ij} = \langle B_i B_j \rangle - \langle B_i \rangle \langle B_j \rangle \tag{5}$$

The indexes i,j represent the field components. The matrix m_{ij} is symmetric with real eigenvalues λ_1, λ_2 and λ_3 and orthogonal eigenvectors $(\hat{X}_{MV}, \hat{Y}_{MV}, \hat{Z}_{MV})$, which represent the directions of minimum, maximum and intermediate variation of the magnetic field (the symbol "^" on top of a variable means that it is a unit vector). The eigenvalues provide the corresponding variance σ_n^2 associated with each direction. Thus, from the eigenvectors $(\hat{X}_{MV}, \hat{Y}_{MV}, \hat{Z}_{MV})$, it is possible to construct the rotation matrix $\boldsymbol{T}$ such that the components of the field in the MV frame of reference can be written as

$$B_{MV} = T \cdot B \tag{6}$$

We will call $B_{X_{MV}}$ the field component that corresponds to $\hat{X}_{MV}$ (Minimum Variance direction), $B_{Y_{MV}}$ to that of the maximum variance direction, and $B_{Z_{MV}}$ to that having the intermediate variance.

2.2. Cylindrical linear force-free model for MCs

The local magnetic structure of MCs at 1 AU has been frequently modeled as a cylindrical linear force-free field (Lundquist, 1950) by several authors (see e.g., Burlaga, 1988; Lepping et al., 1990; Lynch et al., 2003; Dasso et al., 2005b; Gulisano et al., 2005). In this case, the magnetic field is given by

$$\mathbf{B} = B_\phi \hat{\Phi} + B_Z \hat{z} + B_r \hat{r} = B_0 [J_1(\alpha r)\hat{\Phi} + J_0(\alpha r)\hat{z}] \tag{7}$$

where J_n is the Bessel function of the first kind of order n, B_0 is the strength of the axial field at the cloud axis (i.e., at $r = 0$), and α is a constant, such that the twist of the magnetic field lines near the cloud axis turns out to be

$$\tau_0 = \tau(0) = \alpha/2 \tag{8}$$

The gauge-independent magnetic helicity per unit length (L) for this model is (Dasso et al., 2003)

$$\frac{H_r}{L} = \frac{\pi B_0^2 R^2}{\tau_0} \left(J_0^2(2\tau_0 R) + J_1^2(2\tau_0 R) - \frac{J_0(2\tau_0 R)J_1(2\tau_0 R)}{R\tau_0} \right), \tag{9}$$

where R is the radius of the MC.

The magnetic flux across a surface transverse to the cloud axis (that is, with a normal along the $\hat{z}$ axis of the cylindrical structure) is

$$F_z = \frac{\pi B_0 R J_1(2R\tau_0)}{\tau_0} \tag{10}$$

The flux per unit length across a surface defined by the radial direction and the axis of the cloud (i.e., a surface with a normal pointing along the $\hat{\Phi}$ direction) is (see e.g., Mandrini et al., 2005)

$$\frac{F_\phi}{L} = \frac{B_0[1 - J_0(2R\tau_0)]}{2\tau_0} \tag{11}$$

2.3. Minimum Variance method applied to magnetic clouds

The large and coherent rotation of the magnetic field vector observed by the spacecraft when $p \sim 0$, allows us to associate: (1) the large scale maximum variance direction to the azimuthal direction (variation of the observed component of the field of the order of 2 B_0, see B_ϕ in Eq. (7)), (2) the minimum variation to the radial direction (the variance will be close to zero, see B_r in Eq. (7)), and (3) the intermediate variance to the axial direction (variation of the order of B_0, see B_z in Eq. (7)) (see e.g., Bothmer and Schwenn, 1998).

However in Lundquist's model, as well as in the observations of real clouds, the modulus of the magnetic field does not remain constant, being maximum near the cloud axis and minimum toward the cloud boundaries. Moreover, for MCs in expansion and due to magnetic flux conservation in the expanding parcels of fluid, |**B**| can decrease significantly while the spacecraft observes the cloud (see e.g., Berdichevsky et al., 2003; Dasso et al., in press). This decrease of |**B**| with time is called the 'aging' effect since the in situ observations are done at a time, which is more distant from the launch time as the spacecraft crosses the MC. This decrease of |**B**| can affect significantly the result of the MV method. However, the relevant information to find the cloud orientation is in the rotation of the magnetic field. Thus, to decouple the variation of |**B**| from the rotation, we apply the MV technique to the normalized field vector series: $\mathbf{b}(t) = \mathbf{B}(t)/|\mathbf{B}(t)|$.

Because MV does not give the positive sense of the variance directions, we choose this sense for $\hat{X}_{MV}$ so that it makes an acute angle with the Earth–Sun direction ($\hat{X}_{GSE}$). We also choose $\hat{Z}_{MV}$ so that $B_{Z_{MV}}$ is positive at the cloud axis, and $\hat{Y}_{MV}$ is closing the right handed system of coordinates.

3. Generation of synthetic clouds

To generate the set of synthetic MCs we use Lundquist's model to represent their magnetic configuration. The input parameters for this model are: $B_0 = 20$ nT, $\alpha = 2.4/R$ (i.e., we set the MC boundary in coincidence with αR equal to the first zero of the Bessel function of order zero), and $R = 0.1$ AU. The cloud velocity is set to 300 km/s. This is only used to construct the magnetic field time series that an observer located at the Lagrangian point $L1$ would measure in Geocentric Solar Ecliptic (GSE) coordinates (the value of the velocity is not affecting the results). Once the magnetic field model and cloud velocity are fixed, the set

of different clouds is generated taking different values for p and different orientations with respect to the GSE system of coordinates. The set of cloud orientations are given by the angles: θ (latitude angle, the angle between the cloud axis and the ecliptic plane), and φ (longitude angle, the angle between the projection of the cloud axis on the ecliptic plane and the Earth–Sun direction ($\hat{X}_{GSE}$), measured counterclockwise).

The intrinsic cloud reference system and the GSE system of coordinates can be related using the following rotation matrices:

$$\begin{pmatrix} \hat{X}_{cloud} \\ \hat{Y}_{cloud} \\ \hat{Z}_{cloud} \end{pmatrix} = \mathbf{R_2} \cdot \mathbf{R_1} \cdot \begin{pmatrix} \hat{X}_{GSE} \\ \hat{Y}_{GSE} \\ \hat{Z}_{GSE} \end{pmatrix} \tag{12}$$

where

$$\mathbf{R_1} = \begin{pmatrix} \sin\theta\cos\varphi & \sin\theta\sin\varphi & -\cos\theta \\ -\sin\varphi & \cos\varphi & 0 \\ \cos\theta\cos\varphi & \cos\theta\sin\varphi & \sin\theta \end{pmatrix} \tag{13}$$

and

$$\mathbf{R_2} = \begin{pmatrix} \cos\delta & \sin\delta & 0 \\ -\sin\delta & \cos\delta & 0 \\ 0 & 0 & 1 \end{pmatrix}. \tag{14}$$

Without loosing generality we choose δ (the angle of an arbitrary rotation in the plane $(\hat{X}_{cloud}, \hat{Y}_{cloud})$) such that $\hat{X}_{GSE} \cdot \hat{Y}_{cloud} = 0$, that is

$$\tan\delta = \frac{-\tan\varphi}{\sin\theta} \tag{15}$$

Thus, in this case, the spacecraft trajectory in the MC frame turns out to be

$$\mathbf{r}(t) = d(t)\hat{X}_{GSE} + p\hat{Y}_{cloud} \tag{16}$$

with

$$d(t) = -V_{cloud}\frac{\Delta t}{2} + V_{cloud}(t - t_0) \tag{17}$$

where $d(t)$ is the 'signed' distance traveled by the spacecraft within the cloud, this quantity is taken negative when the spacecraft is approaching the cloud axis and positive when it is leaving the cloud center, and $\Delta t = (t_f - t_0)$ is the total transit time (with t_0 and t_f the time at which the spacecraft enters and leaves the structure, respectively).

The projection of the trajectory on the plane $(\hat{X}_{cloud}, \hat{Y}_{cloud})$, which is the polar coordinate $\rho(t)$, is

$$\rho(t) = \sqrt{\left[\left(X(t)_{cloud} \right)^2 + \left(Y(t)_{cloud} \right)^2 \right]} \tag{18}$$

where

$$\begin{cases} X(t)_{cloud} = d(t)(\cos\delta\sin\theta\cos\varphi - \sin\delta\sin\varphi) \\ Y(t)_{cloud} = p = \text{constant} \end{cases}; \tag{19}$$

then, the angle (φ_{sat}) between the projection of the trajectory on the plane $(\hat{X}_{cloud}, \hat{Y}_{cloud})$ and the $\hat{X}_{cloud}$ satisfies

$$\sin\varphi_{sat} = \frac{Y(t)_{cloud}}{|\rho(t)|}$$
$$= \frac{p}{\sqrt{d(t)^2(\cos\delta\sin\theta\cos\varphi - \sin\delta\sin\varphi)^2 + p^2}} \tag{20}$$

$$\cos\varphi_{sat} = \frac{X(t)_{cloud}}{|\rho(t)|}$$
$$= \frac{d(t)(\cos\delta\sin\theta\cos\varphi - \sin\delta\sin\varphi)}{\sqrt{d(t)^2(\cos\delta\sin\theta\cos\varphi - \sin\delta\sin\varphi)^2 + p^2}} \tag{21}$$

The magnetic field time series inside the synthetic cloud is

$$\mathbf{B}(t) = B_0 J_0(\alpha\rho(t))\hat{Z}_{cloud} + B_0 J_1(\alpha\rho(t))\hat{\varphi}_{sat}(t), \tag{22}$$

where $\hat{\varphi}_{sat}(t)$ is related to $\sin\varphi_{sat}$ and $\cos\varphi_{sat}$ as

$$\hat{\varphi}_{sat}(t) = -\sin\varphi_{sat}(t)\hat{X}_{cloud} + \cos\varphi_{sat}(t)\hat{Y}_{cloud}. \tag{23}$$

Note that to compute $\mathbf{B}(t)$ we need $\rho(t)$ and consequently $d(t)$ and Δt (see Eqs. (17) and (18)). To compute Δt, we set $t = t_f$ (or equivalently $t = t_0$) in Eqs. (17) and (18), so that $\rho = R$, then we find

$$\Delta t = \frac{2\sqrt{R^2 - p^2}}{V_{cloud}(\cos\delta\sin\theta\cos\varphi - \sin\delta\sin\varphi)} \tag{24}$$

To obtain the time series of $\mathbf{B}(t)$ from Eq. (22) we take p/R from 0 to 0.9 and the following sets of orientations: $(\theta, \varphi) = (45, 90)(60, 80)(70, 90)(80, 105)(89, 120)$ (the axis of the MC from 45° to almost parallel to $\hat{Z}_{GSE}$ and almost perpendicular to the Sun–Earth line), $(\theta, \varphi) = (5, 200)(30, 180)$ (the cloud axis almost on the ecliptic plane and in the Sun–Earth direction), $(\theta, \varphi) = (0, 90)(10, 270)$ (the cloud axis almost on the ecliptic and perpendicular to the Sun–Earth line), and $(\theta, \varphi) = (10, 130)$.

4. Analysis of synthetic clouds

4.1. General results

From the time series of $\mathbf{B}(t)$ (Eq. (22)), a given orientation and p, we generate the corresponding time series (in the GSE components), which emulates the observations of the spacecraft (i.e., the 'observations' of the synthetic cloud). We then apply the MV technique to the normalized field vectors ($\mathbf{b}(t) = \mathbf{B}(t)/|\mathbf{B}(t)|$) of these synthetic time series.

We estimate the MC orientation: the latitude angle (θ_{MV}) and the longitude angle (φ_{MV}), which for $p \neq 0$ will be different from the correct values of θ and φ chosen at the end of Section 3. From Eq. (24), using V_{cloud} and Δt, we estimate the radius (R_{MV}) assuming that p is null (since it is unknown).

Siscoe and Suey (1972) proposed a criterion to determine the anisotropy of a given normalized vector series $\mathbf{v}^k$, computing the eigenvalues (λ) and the eigenvectors of the matrix $M_{ij} = \langle v_i v_j \rangle$. For a set of 100 vectors, as used in our case, they found a significance criterion to determine

if the set presents significantly distinct spatial directions. This criterion is $\lambda_{min}/\lambda_{int} < 0.72$ and $\lambda_{max}/\lambda_{int} > 1.37$ (a fully random series of vectors satisfies it in 95% of the cases). For the vector series corresponding to the MC field ($\mathbf{b}^k$), the Minimum Variance method finds eigenvalues and eigenvectors of the matrix $m_{ij} = \langle b_i b_j \rangle - \langle b_i \rangle \langle b_j \rangle$ (see Section 2.1).

Upper (lower) panel of Fig. 1 *left* shows the ratio between the minimum and intermediate (maximum and intermediate) eigenvalues obtained from MV (using m_{ij}) applied to the set of the generated synthetic MCs, as a function of p/R. Note that, as expected, these eigenvalues ratios do not depend on the orientation of the cloud (because the eigenvalues are invariant under rotations). λ_{min} stays lower than $5 \times 10^{-4} \lambda_{int}$, while λ_{max} stays above $5\lambda_{int}$.

Fig. 1 *right* shows eigenvalues ratios using the matrix M_{ij} (as done by Siscoe and Suey), where we take $\mathbf{v}^k = \mathbf{b}^k$. Notice that the criterion of Siscoe and Suey is very well satisfied for large values of p/R, and the eigenvalue separation becomes even larger for increasing values of p/R. However, this only assures well distinct variance directions, but it does not measure how good is the approximation of the MC axis by the intermediate eigenvalue direction. The criterion of Siscoe and Suey is only a necessary condition, far from being sufficient for a good determination of the MC orientation.

4.2. Comparison with the expected cloud orientations

In Fig. 2 we report the angle η between the generated cloud axis ($\hat{Z}_{cloud}$) and the one obtained by MV ($\hat{Z}_{MV}$), as a function of p/R, we plot only one curve since η does not depend on the MC orientation. It can be seen that the deviation from the real generated orientation increases with p/R. For $p/R \sim 0.2$, we obtain $\eta \sim 2°$ and when p/R reaches the extreme value ~ 0.9, we get $\eta \sim 18°$. We remark that for real observations, cases with $p/R \sim 0.9$ will be more affected by the interaction between the MC and the
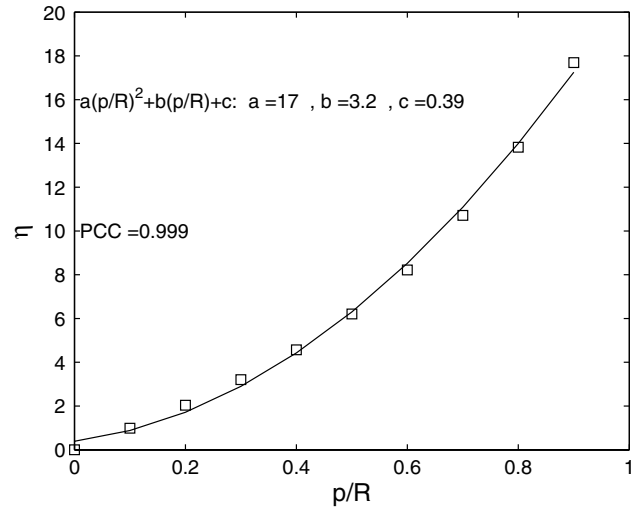
Fig. 2. Angle η between the generated cloud axis ($\hat{Z}_{cloud}$) and the one obtained by MV (squares) as a function of p in units of the MC radius together with the quadratic regression curve (solid line).

solar wind (see e.g., Dasso et al., 2005a) with a consequent observation of $\mathbf{B}(t)$ significantly different from the ideal modeled magnetic configuration; this will introduce biases which are not present in our synthetic MC set.

The deviation angle η is well represented by a quadratic curve (Fig. 2) since the PCC (Pearson correlation coefficient) is 0.999. It is noteworthy that this deviation in the MC orientation is not evident from the eigenvalues ratios (Fig. 1) discussed in the previous section. Despite the MV technique finds well distinguished (minimum, maximum, and intermediate) directions, when p/R is not small those directions do not correspond to $\hat{X}_{cloud}, \hat{Y}_{cloud}, \hat{Z}_{cloud}$.

We compared the above results to those of an analysis using the time series $\mathbf{B}(t)$, so without normalization, and we found worse orientations ($\eta \sim 20°$ for $p/R \sim 0.5$ and $\eta \sim 35°$ for $p/R \sim 0.9$). Thus, we conclude that to get better estimations for the cloud axis orientation it is convenient to apply the MV technique to the normalized time series $\mathbf{b}(t)$.
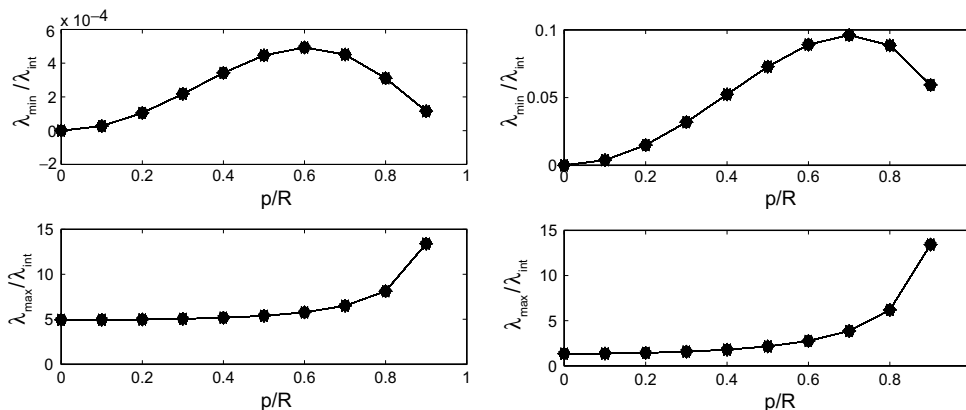
Fig. 1. Left: upper (lower) panel shows the ratio between the minimum and intermediate (maximum and intermediate) eigenvalues from MV (using m_{ij}) for the set of generated MCs as a function of p in units of the MC radius. Right: upper (lower) panel shows the ratios but now using the matrix M_{ij}, where we take $\mathbf{v}^k = \mathbf{b}^k$ for the set of generated MCs.

In Fig. 3 (Fig. 4) we report the deviation in the angles θ (φ), as $\Delta\theta = \theta - \theta_{MV}(\Delta\varphi = \varphi - \varphi_{MV})$. We report these deviations, in addition to the deviation η, since θ and φ are frequently used in the literature to give the orientation of MCs.

There is a general trend to obtain larger deviations in φ than in θ, especially when $|\theta|$ is large (this is an effect of the spherical coordinates used close to where φ is singular, at the two poles). As expected, $|\Delta\theta|$ and $|\Delta\varphi|$ increase as p increases, but with a different behavior for different cloud orientations, which is quantified in Figs. 3 and 4. For all the synthetic MCs $\theta_{MV} < \theta$; thus, MV tends to give lower values of the latitude angle as p increases.

When the cloud axis is close to the ecliptic plane and it is perpendicular to the Sun–Earth direction, θ is very well determined even for very large values of p (see symbols $\triangleleft$ and $\circ$ in Fig. 3). However, clouds with their axis either nearly perpendicular to the ecliptic (see symbols: $\times$ ($\theta = 89$), $\triangleright$ ($\theta = 80$), $\square$ ($\theta = 70$), and $+$ ($\theta = 60$) in Fig. 3) or nearly parallel to Sun–Earth direction (see symbols: $\odot$ ($\varphi = 180$), $\star$ ($\varphi = 200$) in Fig. 3) give the largest errors, e.g., $\Delta\theta$ between $\sim2°$ and $10°$ for $p/R \sim 0.7$.

For the cloud axis close to the Sun–Earth direction and low latitudes, φ is well determined even for very large values of p (see symbol: $\odot$ ($\varphi = 180$) in Fig. 4). For increasing values of the latitude, errors in φ turn to be larger (see symbols: $+$ ($\theta = 60$), $\square$ ($\theta = 70$), $\triangleright$ ($\theta = 80$), and $\times$ ($\theta = 89$) in Fig. 4). We remark that the largest error in the determination of φ, when θ is 89° (cloud axis almost pointing to the ecliptic north), is not meaningful because it comes from the small differences in the determination of $\hat{Z}_{cloud}$ (small η) and, consequently, large deviations in its projection on the ecliptic plane (i.e., on φ). For latitudes lower than $\theta \sim 45°$ we obtain a $\Delta\varphi < 20°$, even for p/R as large as 0.9.

4.3. Comparison with the expected cloud parameters and global magnitudes

To compare with the generated MCs, we fit the physical parameters of Lundquist's model to the $\boldsymbol{B_{MV}}$ components, using a non-linear least-squares fitting, as described in Dasso et al. (2006). Then, from the fitted parameters, we calculate Hr/L and the fluxes as discussed below.

We compute the mean value of $B_{X_{MV}}$, which is expected to be zero in the case $p = 0$, we depict $|\langle B_{X_{MV}}\rangle|/B_{0MV}$ versus p/R in the upper panel of Fig. 5, together with the quadratic regression curve that best fits the points. The devia-
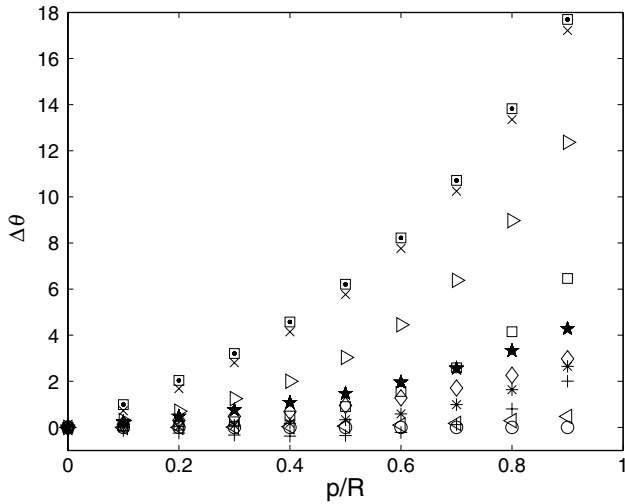

Fig. 3. Bias from Minimum Variance in θ ($\Delta\theta = \theta - \theta_{MV}$) in function of p in units of the radius. Different orientations of the synthetic clouds are represented by $(\theta, \varphi) = *$ $(45, 90)$, $\times$ $(89, 120)$, $+$ $(60, 80)$, $\circ$ $(0, 90)$, $\square$ $(70, 90)$, $\diamond$ $(10, 130)$, $\star$ $(5, 200)$, $\odot$ $(30, 180)$, $\triangleleft$ $(10, 270)$, $\triangleright$ $(80, 105)$.
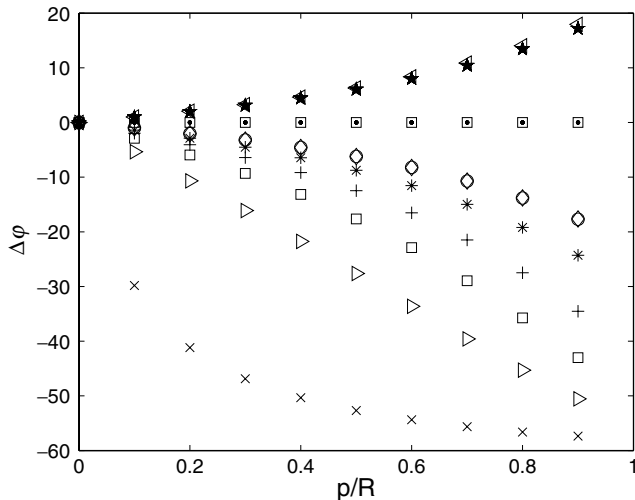

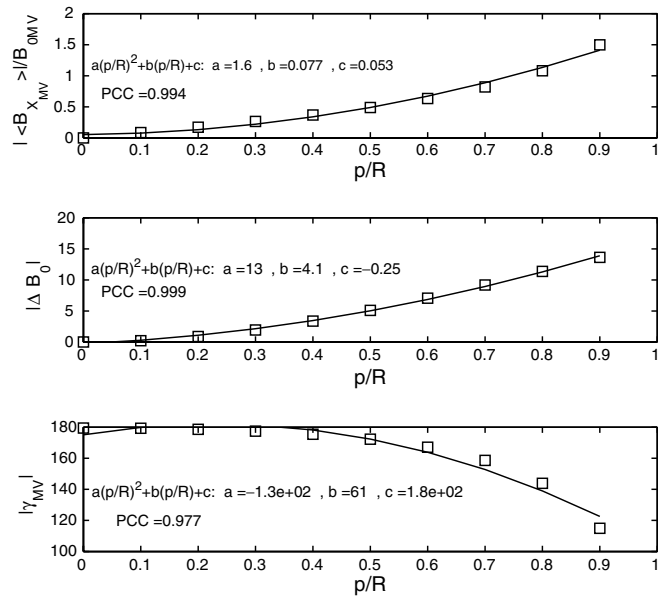Fig. 4. Idem Fig. 3 but showing the difference in φ ($\Delta\varphi = \varphi - \varphi_{MV}$).

Fig. 5. Upper panel: $|\langle B_{X_{MV}}\rangle|/B_{0MV}$. Middle panel: $\Delta B_0 = B_0 - B_{0MV}$. Lower panel: absolute value of the rotation angle of $\mathbf{B}$ in the plane of maximum variance ($|\gamma_{MV}|$). All the quantities are plotted, in function of p in units of the radius. Their quadratic regression curves are added.

tion is larger when p increases. This deviation can provide a quantitative estimation of the impact parameter by reporting the measured value of $\Delta b_x = |\langle B_{X_{MV}} \rangle|/B_{0MV}$ in the upper panel of Fig. 5, or simply by using the approximation $p \sim R\sqrt{\Delta b_x/1.6}$ from the quadratic fit.

The magnetic field strength B_{0MV}, found by fitting Lundquist's model, is also affected by the error introduced by MV in the axis orientation. The middle panel of Fig. 5 shows the difference $\Delta B_0 = B_0 - B_{0MV}$. We also find a quadratic dependence with p/R. The difference in the field strength can be significant, for example $\approx 50\%$ for $p/R = 0.5$.

We also analyze the magnitude of the coherent rotation of the magnetic field as defined by the angle γ between the field vector components that lie on the maximum variance plane ($B_{Z_{MV}}, B_{Y_{MV}}$), taken at the front and end boundaries of the MC. If the right cloud orientation is used, $\gamma = 180°$ for all values of p because all the synthetic clouds satisfy $B_z = 0$ at the MC boundary. However, with the orientation found with the MV method, $|\gamma|$ decreases as p/R increases due to a mix of field components (lower panel of Fig. 5). Thus, we find that the angle $|\gamma|$ varies from $180°$ (for $p = 0$) to $\approx 120°$ in the extreme case when $p = 0.9R$ (i.e., when the spacecraft crosses the cloud close to its periphery). This is still a large coherent rotation of the magnetic field.

Finally, in all panels of Fig. 5 we plot only a unique curve to represent all the synthetic clouds for a given p/R, since the values obtained do not depend on the MC orientation.

Fig. 6 shows the radius obtained from MV (assuming $p = 0$) in units of the model radius ($R = 0.1$ AU) as a function of p/R; thus, it quantifies the underestimation of the real radius using R_{MV} when $p \neq 0$. The solid line in this figure corresponds to $\sqrt{(1 - (p/R)^2)}$, the value that would be obtained for the correct orientations defined for the

synthetic clouds, but with the (only) bias given when the underestimation of the size is due to the finite value of p. This introduces an error in the cloud radius lower than 30% for $p/R < 0.7$. As expected, the only cases having significant variations in the estimated radius because of errors in the orientations are those where the cloud axis is nearly parallel to the Sun–Earth direction: symbols $\diamond$ ($\theta = 10°, \varphi = 130°$), $\boxdot$ ($\theta = 30°, \varphi = 180°$), and $\star$ ($\theta = 5°, \varphi = 200°$).

Fig. 7 shows the fitted values for α (α_{MV}). As expected, the value $\alpha = 24$ AU^{-1} (used for all the synthetic clouds) is recovered when $p/R = 0$. The solid line represents $\alpha = 24$ AU$^{-1}/\sqrt{1 - (p/R)^2}$, which corresponds to the value of α that cancels $J_0(\alpha R)$ for the underestimated radius $\sqrt{R^2 - p^2}$. Except for the same three MCs that give the largest error in R (axis oriented near the Sun–Earth direction), the obtained values of α differ from $\alpha = 24$ AU^{-1} basically due to the underestimation of the radius. The right panel of Fig. 7 shows that, excluding the three cases mentioned before, there is a small trend to cancel this effect, because the fitted values of α are between

$\alpha = 24$ AU^{-1} and $\alpha = 24$ AU$^{-1}/\sqrt{(1 - (p/R)^2)}$.

For every synthetic cloud we compute the magnetic helicity (Eq. (9)) from the model and the fitted parameters to the Lundquist's model, using the MV orientation (H^{MV}). In Fig. 8 we plot $\Delta H/H = \frac{H - H^{MV}}{H}$ as a function of p/R. The solid line corresponds to the helicity computed with the correct (values used to the produce the synthetic clouds) $B_0(=20$ nT) and $\alpha(=24$ AU^{-1}), but considering the underestimated radius as $\sqrt{R^2 - p^2}$. H^{MV} underestimates H for two reasons: (1) the underestimation of the radius and (2) the bias introduced in the fitted values of B_{0MV} and α_{MV}. The radius underestimation can be partially corrected by estimating the impact parameter from the observed
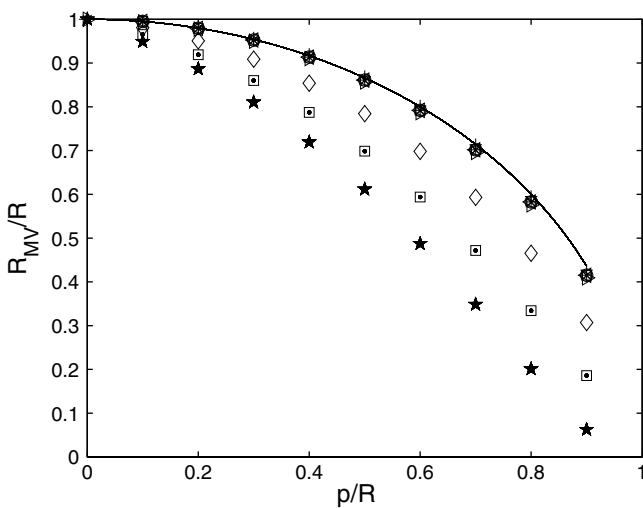

Fig. 6. R_{MV} in units of the synthetic radius R (=0.1 AU) as a function of p/R. Solid line corresponds to the small expected radius (because of the assumption $p = 0$) computed from the orientations of the synthetic MCs. Symbols are given as in Fig. 3.
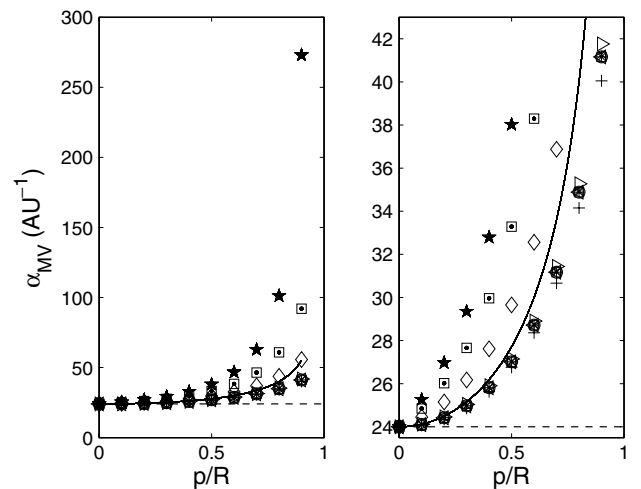

Fig. 7. α_{MV} as a function of p/R. Dashed line corresponds to the value set to generate the synthetic clouds ($\alpha = 24$ AU^{-1}). The symbols for different orientations are given as in Fig. 3. Solid line shows $\alpha = 24$ AU$^{-1}/\sqrt{(1 - (p/R)^2)}$. The left panel shows the full set of clouds, while the right panel shows a zoom.
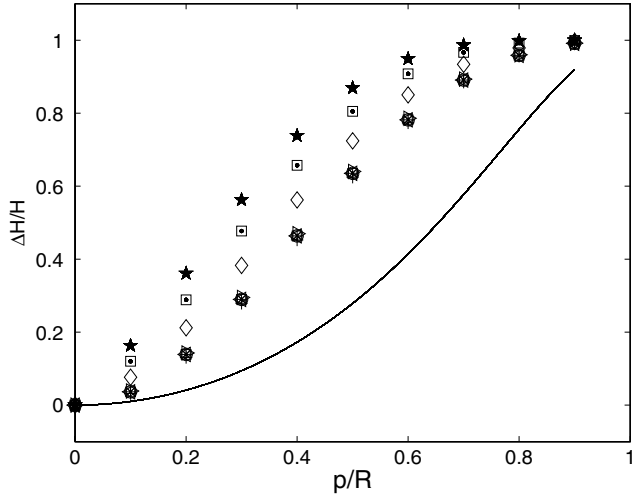
Fig. 8. Difference between the theoretical and estimated values (using MV) of the magnetic helicity, divided by the theoretical value, $\Delta H/H = (H - H^{MV})/H$, as a function of p/R. The symbols for different orientations are given as in Fig. 3. Solid line corresponds to H^{MV} computed with the values for B_0 and α used to generate the synthetic MCs, $B_0 (=20\ nT)$ and $\alpha (=24\ AU^{-1})$, but considering the radius $\sqrt{(R^2 - p^2)}$.

$|\langle B_{X_{MV}} \rangle| / B_{0MV}$ (upper panel of Fig. 5), but an underestimation remains due to the error in the MC orientation (Fig. 7). Indeed, from the middle panel of Fig. 5 (underestimation of B_0 for finite values of p) and (Fig. 7) (overestimation of α), and the main dependence on these two parameters (Eq. (9)), it is expected that H_{MV} will be further underestimated. If the cloud size is corrected, the largest error is $\approx 30\%$ for $p/R \approx 0.5$. Thus, the largest source of error (always an underestimation) in the magnetic helicity value of ideal MCs is the influence of p on the estimation of the radius.

We also compute $\Delta F_z/F_z = \frac{F_z - F_z^{MV}}{F_z}$ (Fig. 9) and $\Delta F_\phi/F_\phi = \frac{F_\phi - F_\phi^{MV}}{F_\phi}$ (Fig. 10). Both fluxes have the same sources of underestimation as the magnetic helicity above.
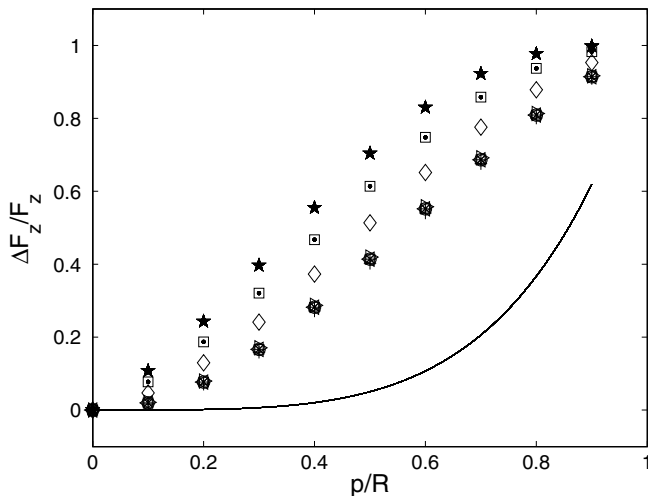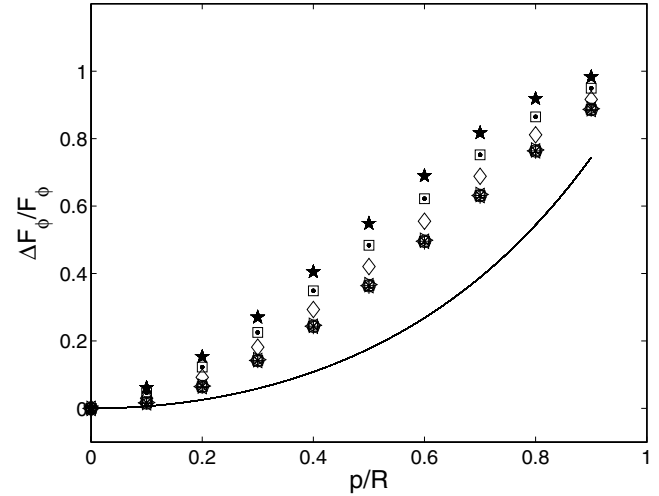

Fig. 9. Idem as Fig. 8 but for F_z values.

Fig. 10. Idem as Fig. 8 but for F_ϕ/L values.

From the above results, we conclude that the main reason for underestimations of global quantities is the decrease of R_{MV}, which can be corrected if p is computed. We also note that for the three global quantities, the largest deviations appear in clouds oriented with their axes close to the Earth–Sun direction.

5. Summary and conclusions

We study the bias introduced by the Minimum Variance (MV) technique in the determination of the orientation and size of magnetic clouds (MCs). We also analyze the influence of this bias and fitted parameters on the estimation of their global quantities (magnetic fluxes and helicity) for non-negligible values of the impact parameter p compared to the MC radius R.

We explore this bias studying a set of synthetic cylindrical and linear force-free field MCs. The physical parameters for this model are chosen to be the same for all clouds and the only differences in the set correspond to different orientations and impact parameters (p/R).

MCs can present signatures of strong expansion (an effect not considered in our synthetic set of MCs) (e.g., Shimazu and Marubashi, 2000; Berdichevsky et al., 2003; Nakwacki et al., 2005, 2006). However, the main source of error when using MV for expanding MCs is introduced by the strong decrease of |**B**|. This effect can be corrected if MV is applied to the normalized time series: $\mathbf{b}(t) = \mathbf{B}(t)/|\mathbf{B}(t)|$. Moreover, Dasso et al. (in press) compared the orientation of an MC using the normalized MV technique with another technique that considers flux cancellation (Dasso et al., 2006). Both methods were in a good agreement. However, other effects can introduce biases on the MC orientation and size. Examples are the deviation from a cylindrical symmetry, ambiguous MC boundaries, or the presence of a significant level of field fluctuations. Such effects are not studied in the present work. This will be the purpose of a future research.

We quantify, in function of p, the dependence of the increasing deviation (η) of the MC symmetry axis ($\hat{Z}_{\text{cloud}}$), provided by MV applied to the normalized series of vectors, from the generated one. We find a deviation of $\eta \sim 3°$ for $p \sim 30\%$ of the cloud radius; even more, η remains being lower than $20°$ for p as high as 90% of the MC radius. When MV is applied to $\mathbf{B}(t)$ we obtain larger deviations; thus, we conclude that application of MV to $\mathbf{b}(t)$ gives better results.

The criterion discussed in Siscoe and Suey (1972), based on the quantification of the eigenvalue ratios, is a good estimator to determine if a given vector set corresponds to well distinguished spatial directions. This criterion has been used in the literature to validate the goodness of the orientations given by MV. However, we have found that even when this criterion is very well satisfied, the MV directions can still deviate significantly from the main cloud axes. Thus, this criterion is not a good estimator of the quality of the cloud orientation obtained with the MV method. We conclude that this criterion should be taken with care, since to have well distinguished variance directions is a necessary but far from sufficient condition to assure that the orientation found is the real MC orientation.

A good determination of the latitude (θ) and longitude (φ) of the main axis of the MC is important to obtain a good estimation of the cloud size from its speed and range of observed times. We have found that θ is better determined for an MC with its axis nearly on the ecliptic plane (i.e., $\theta \sim 0°$) and nearly perpendicular to the Sun–Earth direction ($\varphi \sim 0°$ or $\varphi \sim 180°$), even for values of p as large as $p \sim 0.9$ (see Fig. 3). For all the studied cases we have found typically $\Delta\theta$ lower than $5°$ even for p/R as large as 0.9. The worse determination of φ corresponds to the MC axis nearly perpendicular to the ecliptic plane ($\theta \sim 90°$), being this large uncertainty in φ a geometric amplification due to the description of the poles in spherical coordinates (the full range of φ values are clustered around the poles).

One of the main unknown parameters of an MC is its radius, which can be significantly underestimated from observations when p is a significant fraction of the MC radius. This implies an underestimation of extensive global magnetohydrodynamical quantities in MCs, as the magnetic fluxes and helicity. The deviation from zero of the mean value of the $\hat{X}_{MV}$ magnetic field component (in the direction of lowest variance) can be used to obtain a first order estimation of p, directly from observations, as $p \sim R\sqrt{\Delta b_x/1.6}$ for Lundquist's MCs. This estimation of p lets us improve the estimation of the MC radius and, consequently, the estimations of global quantities since the uncertainty in the cloud size is one of the main sources of error.

Acknowledgements

References

Attrill, G., Nakwacki, M.S., Harra, L.K., van Driel-Gesztelyi, L., Mandrini, C.H., Dasso, S., Wang, J. Using the evolution of coronal dimming regions to probe the global magnetic field topology. Solar Physics 238, 117–139, 2006.

Berdichevsky, D.B., Lepping, R.P., Farrugia, C.J. Geometric considerations of the evolution of magnetic flux ropes. Physical Review E 67 (3), 036405, 2003.

Bothmer, V., Schwenn, R. The structure and origin of magnetic clouds in the solar wind. Annales Geophysicae 16, 1–24, 1998.

Burlaga, L.F. Magnetic clouds and force-free fields with constant alpha. Journal of Geophysical Research 93 (12), 7217–7224, 1988.

Burlaga, L.F. Interplanetary Magnetohydrodynamics. Oxford University Press, New York, 1995.

Burlaga, L.F., Behannon, K.W. Magnetic clouds: voyager observations between 2 and 4 AU. Solar Physics 81, 181–192, 1982.

Burlaga, L., Fitzenreiter, R., Lepping, R., Ogilvie, K., Szabo, A., Lazarus, A., Steinberg, J., Gloeckler, G., Howard, R., Michels, D., Farrugia, C., Lin, R.P., Larson, D.E. A magnetic cloud containing prominence material – January 1997. Journal of Geophysical Research 103, 277, 1998.

Cid, C., Hidalgo, M.A., Nieves-Chinchilla, T., Sequeiros, J., Viñas, A.F. Plasma and magnetic field inside magnetic clouds: a global study. Solar Physics 207, 187–198, 2002.

Dasso, S., Mandrini, C.H., Démoulin, P., Farrugia, C.J. Magnetic helicity analysis of an interplanetary twisted flux tube. Journal of Geophysical Research (Space Physics) 108 (A10), 1362–1364, 2003.

Dasso, S., Gulisano, A.M., Mandrini, C.H., Démoulin, P. Model-independent large scale magnetohydrodynamic quantities in magnetic clouds. Advances in Space Research 35, 2172–2177, 2005a.

Dasso, S., Mandrini, C.H., Démoulin, P., Luoni, M.L., Gulisano, A.M. Large scale MHD properties of interplanetary magnetic clouds. Advances in Space Research 35, 711–724, 2005b.

Dasso, S., Mandrini, C.H., Démoulin, P., Luoni A new model-independent method to comute magnetic helicity in mangetic clouds. Astronomy & Astrophysics 455, 349–359, 2006.

Dasso, S., Nakwacki, M.S., Démoulin, P., Mandrini, C.H. Progressive transformation of a flux rope to an ICME. Solar Physics, in press.

Farrugia, C.J., Janoo, L.A., Torbert, R.B., Quinn, J.M., Ogilvie, K.W., Lepping, R.P., Fitzenreiter, R.J., Steinberg, J.T., Lazarus, A.J., Lin, R.P., Larson, D., Dasso, S., Gratton, F.T., Lin, Y., Berdichevsky, D. A uniform-twist magnetic flux rope in the solar wind, in: AIP Conference Proceedings 471: Solar Wind Nine, pp. 745–748, 1999.

Goldstein, H. On the field configuration in magnetic clouds, in: Solar Wind Conference, pp. 731–733, November 1983.

Gulisano, A.M., Dasso, S., Mandrini, C.H., Démoulin, P. Magnetic clouds: a statistical study of magnetic helicity. Journal of Atmospheric and Terrestrial Physics 67, 1761–1766, 2005.

Hidalgo, M.A. A study of the expansion and distortion of the cross section of magnetic clouds in the interplanetary medium. Journal of Geophysical Research 108 (A8), 1320, 2003.

Hidalgo, M.A., Cid, C., Medina, J., Viñas, A.F. A new model for the topology of magnetic clouds in the solar wind. Solar Physics 194, 165–174, 2000.

Hidalgo, M.A., Cid, C., Medina, J., Viñas, A.F., Sequeiros, J. A non-force free approach to the topology of magnetic clouds in the solar wind. Journal of Geophysical Research 107, doi:10.1029/2001JA900100, 2002.

Hu, Q., Dasgupta, B. Calculation of magnetic helicity of cylindrical flux rope. Geophysical Research Letters 32, L12109, 2005.

Hu, Q., Sunnerup, B.U.O. Reconstruction of magnetic flux ropes in the solar wind. Geophysical Research Letters 28 (3), 467–470, 2001.

Hu, Q., Sunnerup, B.U.O. Reconstruction of magnetic flux ropes in the solar wind: orientations and configurations. Journal of Geophysical Research 107, 1142–1156, 2002.

Klein, L.W., Burlaga, L.F. Interplanetary magnetic clouds at 1 AU. Journal of Geophysical Research 87, 613–624, 1982.

Lepping, R.P., Burlaga, L.F., Jones, J.A. Magnetic field structure of interplanetary magnetic clouds at 1 AU. Journal of Geophysical Research 95 (14), 11957–11965, 1990.

Lepping, R.P., Berdichevsky, D.B., Ferguson, T.J. Estimated errors in magnetic cloud model fit parameters with force-free cylindrically symmetric assumptions. Journal of Geophysical Research 108, 1356–1375, 2003.

Lepping, R.P., Berdichevsky, D.B., Wu, C.C., Szabo, D., Narock, T., Mariani, F., Lazarus, A.J., Quivers, A.J. A summary of WIND magnetic clouds for years 1995–2003: model-fitted parameters, associated errors and classifications. Annales Geophysicae (24), 215–245, 2006.

Lundquist, S. Magnetohydrostatic fields. Arkiv for Fysik 2, 361–365, 1950.

Lynch, B.J., Zurbuchen, T.H., Fisk, L.A., Antiochos, S.K. Internal structure of magnetic clouds: plasma and composition. Journal of Geophysical Research (Space Physics) 108, 1–6, 2003.

Lynch, B.J., Gruesbeck, J.R., Zurbuchen, T.H., Antiochos, S.K. Solar cycle-dependent helicity transport by magnetic clouds. Journal of Geophysical Research (Space Physics) 110, 8107, 2005.

Mandrini, C.H., Pohjolainen, S., Dasso, S., Green, L.M., Démoulin, P., Van Driel-Gesztelyi, L., Copperwheat, C., Foley, C. Interplanetary flux rope ejected from an Z-ray bright point. The smallest magnetic cloud source-region ever observed. Astronomy & Astrophysics 434, 725–740, 2005.

Mulligan, T., Russell, C.T. Multispacecraft modeling of the flux rope structure of interplanetary coronal mass ejections: Cylindrically symmetric versus nonsymmetric topologies. Journal of Geophysical Research 106, 10581–10596, 2001.

Mulligan, T., Russell, C.T., Anderson, B.J., Lohr, D.A., Toth, B.A., Zanetti, L.J., Acuna, M.H., Lepping, R.P., Gosling, J.T., Luhmann, J.G. Flux rope modeling of an interplanetary coronal mass ejection observed at WIND and NEAR, in: Solar Wind Nine, AIP Conference Proceedings, vol. 471. p. 689, 1999.

Nakwacki, M.S., Dasso, S., Mandrini, C.H., Demoulin, P. Global magnitudes in expanding magnetic clouds, in: Revista Mexicana de Astronomia y Astrofisica Conference Series, pp. 155, 2006.

Nakwacki, M.S., Dasso, S., Mandrini, C.H., Démoulin, P. Helicity analysis for expanding magnetic clouds: a case study, in: Proceedings of Solar Wind 11 – SOHO 16, ESA SP-592, pp. 629–632, 2005.

Riley, P., Linker, J.A., Lionello, R., Mikić, Z., Odstrcil, D., Hidalgo, M.A., Cid, C., Hu, Q., Lepping, R.P., Lynch, B.J., Rees, A. Fitting flux ropes to a global MHD solution: a comparison of techniques. Journal of Atmospheric and Terrestrial Physics 66, 1321–1331, 2004.

Shimazu, H., Marubashi, K. New method for detecting interplanetary flux ropes. Journal of Geophysical Research 105, 2365–2374, 2000.

Siscoe, G.L., Suey, R.W. Significance criteria for variance matrix applications. Journal of Geophysical Research 77 (7), 1321–1322, 1972.

Sonnerup, B.U.O., Scheible, M. Analsyis Methods for Multispacecraft Data. Kluwer Academic, 1998.

Sunnerup, B.U.O., Cahill, L.J. Magnetopause structure and attitude from explorer 12 observations. Journal of Geophysical Research 72 (1), 171–183, 1967.

Vandas, M., Romashets, E.P. A force-free field with constant alpha in an oblate cylinder: a generalization of the Lundquist solution. Astronomy & Astrophysics 398, 801–807, 2003.

Xiao, C.J., Pu, Z.Y., Ma, Z.W., Fu, S.Y., Huang, Z.Y., Zong, Q.G. Inferring of flux rope orientation with the minimum variance analysis technique. Journal of Geophysical Research (Space Physics) 109, 11218–11226, 2004.